

AD-A032 118

NAVAL INTELLIGENCE SUPPORT CENTER WASHINGTON D C TRA--ETC F/G 20/4
LIFT EFFECTIVENESS OF CERTAIN CONFIGURATIONS IN TERMS OF THE TH--ETC(U)
AUG 76 A G SAKHNO, V I KHOLYABKO

UNCLASSIFIED

NISC-TRANS-3833

NL

1 OF 1
AD
A032118



END

DATE
FILMED
1-77



DEPARTMENT OF THE NAVY
NAVAL INTELLIGENCE SUPPORT CENTER
TRANSLATION DIVISION ✓
4301 SUITLAND ROAD
WASHINGTON, D.C. 20390

FG 4

AD A032118

CLASSIFICATION: UNCLASSIFIED

APPROVED FOR PUBLIC RELEASE, DISTRIBUTION UNLIMITED

TITLE:

6 Lift Effectiveness of Certain Configurations in Terms
of the Thin Body Theory ✓

(Nesushchiye svoystva nekotorykh konfiguratsiy po
teorii tonkogo tela) 9

AUTHOR(S): 10 A.G. Sakhno, A.G. and Kholyabko, V.I. ✓

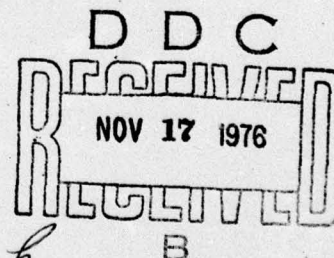
PAGES: 8

SOURCE: Samoletostroyeniye i tekhnika vozdushnogo flota,
No. 21, Khar'kov State University Publishing House,
Khar'kov, 1972
Pages 3-10

ORIGINAL LANGUAGE: Russian

TRANSLATOR: C

NISC TRANSLATION NO. 3833 ✓



APPROVED P.T.K.

DATE 12 August 1976

14 NISC-Trans-3833

11 129 p.

407 682
648

LIFT EFFECTIVENESS OF CERTAIN CONFIGURATIONS IN TERMS OF THE THIN BODY THEORY

[Sakhno, A. G. and V. I. Kholyabko, *Nesushchiye svoystva nekotorykh konfiguratsiy po teorii tonkogo tela*, in: Aircraft Construction and Technology of the Air Fleet (Samoletostroyeniye i tekhnika vozdushnogo flota), No. 21, Khar'kov State University Publishing House, Khar'kov, 1972, pp. 3-10; Russian]

Papers evaluating the aerodynamic characteristics of pyramidal and conical bodies with various cross sections in a hypersonic gas flow have been published recently.^{1,2} Also of definite interest is the analysis of aerodynamic characteristics of such bodies at lower flight velocities, in particular, those corresponding to takeoff and landing conditions. In the present paper, the lift effectiveness of certain configurations is analyzed by use of the thin body theory. /3*

In accordance with this theory, three-dimensional flow past a thin body at a small angle of attack is replaced by a study of two dimensional flow in a plane perpendicular either to the velocity vector of the incident flow or to the longitudinal axis of the body. For thin bodies at small angles of attack, the flow characteristics in such planes are identical. However, it is more convenient to discuss the flow in a plane perpendicular to the longitudinal axis of the body, i.e., to determine the normal force instead of the lift, since in this case the effect of bottom drag, which may be significant for bodies with a developed downstream portion, is ruled out.

In a coordinate system fixed relative to an undisturbed fluid, the flow in this plane is unsteady, owing to a nonuniform motion (for bodies with a rectilinear axis) of the cross sectional contour at velocity $V_\infty \alpha$ and to its expansion. As the flow field increases with the expanding contour, a local normal force $\frac{dN}{dx}$ appears, equal to the product of contour velocity $V_\infty \alpha$ by the local rate of increase in the apparent flow mass $m(x)$ in a direction perpendicular to the longitudinal body axis, i.e.,

$$\frac{dN}{dx} = V_\infty \alpha \frac{dm}{dt} = V_\infty \alpha \frac{dm}{dx} \frac{dx}{dt} = V_\infty^2 \alpha \frac{dm}{dx}.$$

Integrating this expression over the length of the body from the apex to the maximum span section and introducing the derivative of the normal force coefficient with respect to the angle of attack C_n^α , we obtain

$$C_n^\alpha = \frac{2m}{\rho S}. \quad (1)$$

Here m is the apparent mass in the maximum span section, ρ is the density of the medium, and S is the characteristic area.

The apparent mass will be calculated by applying a method based on the use of the theory of a function of a complex variable, in particular, the theory of residues and conformal mapping.³ The formula for determining the apparent mass will be in this case /4

$$m = \rho \operatorname{Re} \left\{ \oint F(z) dz \right\} - \rho S_0. \quad (2)$$

*Numbers in the right margin indicate pagination in the original text.

where $F(z)$ is the complex streaming potential in the transverse plane z during the motion of contour C at unit velocity along the positive direction of the vertical axis in a fluid at rest at infinity; S_0 is the area bounded by contour C (area of the bottom section).

The complex potential $F(z)$ can be determined by conformal mapping of the exterior of the specified contour C onto the exterior of a circle of radius r in the ζ plane. Let this mapping be made by means of the function $z = f(\zeta)$ without changing the conditions at infinity, and let the complex potential of the flow of unit velocity past the circumference in the negative direction of the imaginary axis of the ζ plane be

$$\Phi(\zeta) = i \left(\zeta - \frac{r^2}{\zeta} \right). \quad (3)$$

Then for the function $F(z) + iz$, which obviously describes the flow past a stationary contour C of a fluid moving at unit velocity at infinity in the negative direction of the vertical axis, we obtain

$$F[z(\zeta)] + iz(\zeta) = i \left(\zeta - \frac{r^2}{\zeta} \right),$$

whence

$$F[z(\zeta)] = i[\zeta - z(\zeta)] - i \frac{r^2}{\zeta}.$$

In the transverse z plane, the function $F(z)$ outside contour C is an analytic function; therefore, the integration in formula (2) can be extended to an infinitely large contour, and the real part of the integral may be determined by using Cauchy's residue theorem. This facilitates the solution of the problem, since in calculating the apparent mass it is not necessary to know the complete form of the function $F(z)$, but only to have its expansion for $z \rightarrow \infty$. Since it is required that the flows at infinity in the z and ζ planes not be distorted, the general formula for the transformation $z = f(\zeta)$ will be

$$z(\zeta) = \zeta + \sum_{k=0}^{\infty} \frac{a_k}{\zeta^k}. \quad (4)$$

By Eq. (4), the expression for the complex potential $F[z(\zeta)]$ may be written

$$F[z(\zeta)] = -i \frac{r^2}{\zeta} - i \sum_{k=0}^{\infty} \frac{a_k}{\zeta^k}. \quad (5)$$

Using Eq. (5), we obtain the final formula for the apparent mass

$$m = 2\pi\rho \left[r^2 - \frac{S_0}{2\pi} + \operatorname{Re}(a_1) \right], \quad (6)$$

where $\operatorname{Re}(a_1)$ is the real part of coefficient a_1 of the term $\frac{1}{\zeta}$ in expansion (4).

Let us note a few characteristic features resulting from the above formulas. /5
First, the center of the mapped circle in the ζ plane may be shifted along the imaginary axis, but this will not affect the final form of formula (6). Second, according to Eq. (1), in order to determine the normal force coefficient, it is necessary to know the apparent mass only for the base contour of the body, and the shapes of the intermediate sections do not affect the magnitude of this coefficient. Third, since the absolute value of the apparent mass is independent

of the direction of motion of the body along the vertical axis, in the case of a body with a cross-sectional contour unsymmetric relative to the horizontal axis, the value of the coefficient C_n^α will be the same for the right-side-up and inverted positions of the body.

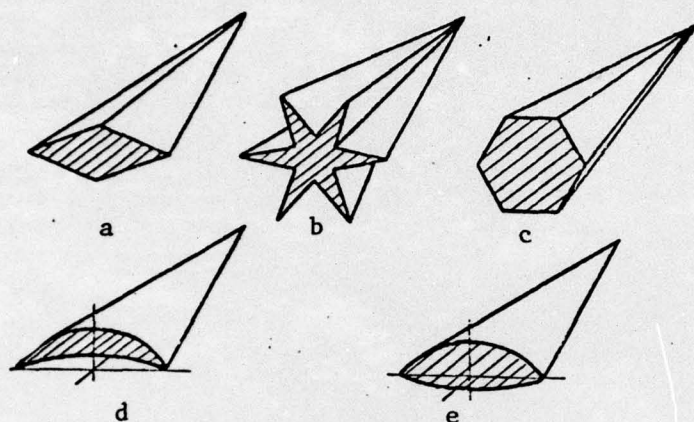


FIGURE 1

ACCESSION for	
RTIS	White Section <input checked="" type="checkbox"/>
DOC	Buff Section <input type="checkbox"/>
UNANNOUNCED	<input type="checkbox"/>
JUSTIFICATION	
BY	
DISTRIBUTION/AVAILABILITY CODES	
Dist.	AVAIL. and/or SPECIAL
A	

The above considerations are applied to an analysis of the lift effectiveness of the configurations shown in Fig. 1. The cross-sectional contours of the bodies are symmetric about the vertical axis, and the projections in the plane of the bodies studied are triangular. The area of this triangle is taken as the characteristic area S in calculating the normal force coefficient. The maximum width (span) of the body L and the area S determine the aspect ratio of the projection of the body in the plane $\lambda = \frac{L^2}{S}$. The pressure center of all the bodies considered, irrespective of the cross-sectional shape in terms of the thin body theory, is located at a distance of $2/3$ length from the nose of the body.

As a first example, we will consider pyramidal bodies whose cross sections are double-wedged (Fig. 1a), regular star-shaped (Fig. 1b) or regular convex (Fig. 1c) polygons. If the half-angle at a vertex of a regular star-shaped polygon with n prongs is $\pi\beta$, then for $\beta = \frac{n-2}{2n}$, a regular convex polygon with n sides, and for $\beta = \frac{n-1}{2n}$, with $2n$ sides is obtained. The rhombus may also be regarded as a special case of a star-shaped polygon with $n = 2$. To avoid exceeding the bounds of the contour of the circumscribed circle, the parameter will be bounded by the following limits: /6

$$0 < \beta \leq \frac{n-1}{2n}.$$

The exterior of contour C of a regular star-shaped polygon is mapped onto the exterior of a circle of radius r by means of the Schwarz-Christoffel formula:⁴

$$z = \int (\zeta^n - r^n)^{1-2\beta} (\zeta^n + r^n)^{2\beta + \frac{2}{n} - 1} \frac{d\zeta}{\zeta^{\frac{1}{n}}}. \quad (7)$$

Expanding Eq. (7) in a series at infinity

$$z = \zeta - \frac{2r^n \left(2\beta + \frac{1}{n} - 1 \right)}{n-1} \frac{1}{\zeta^{n-1}} + \dots \quad (8)$$

we find that $\text{Re}(a_1) = r^2(1 - 4\beta)$ when $n = 2$ and $\text{Re}(a_1) = 0$ when $n \geq 3$.

To determine the radius r of the mapped circle, the following condition will be used: the side of the star-shaped polygon $|z_2 - z_1| = l$ is mapped into an arc of circle $\zeta = re^{i\theta}$ with central angle $\Delta\theta = \frac{\pi}{n}$, i.e.,

$$\begin{aligned} z_2 - z_1 &= 2^{\frac{2}{n}} r e^{(1-\beta)\pi i} \int_0^{\frac{\pi}{n}} \left(\sin \frac{n\theta}{2} \right)^{1-2\beta} \left(\cos \frac{n\theta}{2} \right)^{2\beta + \frac{2}{n} - 1} d\theta = \\ &= 2^{\frac{2}{n}} r e^{(1-\beta)\pi i} B \left(1 - \beta, \frac{1}{n} + \beta \right), \end{aligned}$$

where $B(1 - \beta, \frac{1}{n} + \beta)$ is a beta function.

Considering that*

$$z_2 - z_1 = L \frac{e^{(1-\beta)\pi i}}{2 \left(1 + \frac{\text{tg } \frac{\beta\pi}{n}}{\text{tg } \frac{\pi}{n}} \right) \cos \beta\pi},$$

We obtain the following expression for the radius of the mapped circle:

$$r = L \frac{n}{2^{\frac{2}{n}} \left(1 + \frac{\text{tg } \frac{\beta\pi}{n}}{\text{tg } \frac{\pi}{n}} \right) B \left(1 - \beta, \frac{1}{n} + \beta \right) \cos \beta\pi} \quad (9)$$

Since the area of the bottom section of the bodies studied may be written as

$$S_0 = L^2 \frac{n}{4} \frac{\text{tg } \frac{\beta\pi}{n}}{1 + \frac{\text{tg } \frac{\beta\pi}{n}}{\text{tg } \frac{\pi}{n}}}, \quad (10)$$

then on the basis of formulas (6), (8), (9) and (10), we determine the expressions for the apparent masses of the given sections:

for $n = 2$

$$m = \pi \rho L^2 \left\{ \frac{1 - 2\beta}{\left[B \left(1 - \beta, \frac{1}{2} + \beta \right) \cos \beta\pi \right]^2} - \frac{\text{tg } \beta\pi}{2\pi} \right\}; \quad (11)$$

for $n \geq 3$

$$m = \frac{\pi \rho L^2}{4} \left\{ \frac{2n^2}{\sqrt[3]{16} \left[\left(1 + \frac{\text{tg } \beta\pi}{\text{tg } \frac{\pi}{n}} \right) B \left(1 - \beta, \frac{1}{n} + \beta \right) \cos \beta\pi \right]^2} - \frac{n}{\pi} \frac{\text{tg } \beta\pi}{1 + \frac{\text{tg } \beta\pi}{\text{tg } \frac{\pi}{n}}} \right\}. \quad (12)$$

For the coefficients C_n^α we correspondingly obtain:

for $n = 2$

$$C_n^\alpha = \frac{\pi \lambda}{2} \cdot 4 \left\{ \frac{1 - 2\beta}{\left[B \left(1 - \beta, \frac{1}{2} + \beta \right) \cos \beta\pi \right]^2} - \frac{\text{tg } \beta\pi}{2\pi} \right\}; \quad (13)$$

*Translator's Note: in the display equations, read tg as tan.

for $n \geq 3$

$$C_n^\alpha = \frac{\pi\lambda}{2} \left\{ \frac{2n^2}{\sqrt{16} \left[\left(1 + \frac{\operatorname{tg} \frac{\beta\pi}{n}}{\operatorname{tg} \frac{\pi}{n}} \right) B \left(1 - \beta, \frac{1}{n} + \beta \right) \cos \beta\pi \right]^2} - \frac{n}{\pi} \frac{\operatorname{tg} \beta\pi}{1 + \frac{\operatorname{tg} \frac{\beta\pi}{n}}{\operatorname{tg} \frac{\pi}{n}}} \right\}. \quad (14)$$

To estimate the effect of the thickness of the cross section on the lift effectiveness of the bodies, we will introduce the relative coefficient

$$\bar{C}_n^\alpha = \frac{C_n^\alpha}{C_{n*}^\alpha}, \quad \text{where } C_{n*}^\alpha \text{ is the characteristic of the body under consideration}$$

($n = \text{const}$) for zero thickness of the cross section ($\beta = 0$). For $\beta = 0$, it follows from formulas (13) and (14) that:

for $n = 2$

$$C_{n*}^\alpha = \frac{\pi\lambda}{2}; \quad (15)$$

for $n \geq 3$

$$C_{n*}^\alpha = \frac{\pi\lambda}{2} \frac{2}{\sqrt{16}}. \quad (16)$$

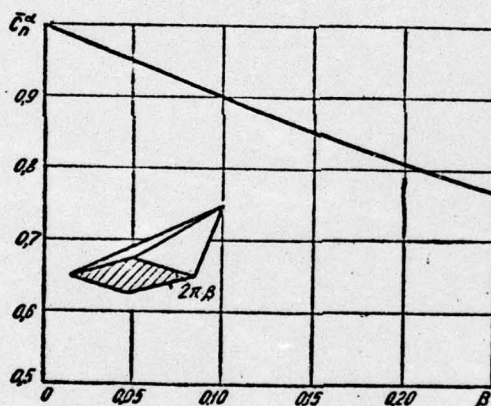


FIGURE 2

Expressions (15) and (16) are the same as the formulas given in Ref. 5. The functions $\bar{C}_n^\alpha = f(\beta)$ for different values of n are given in Figs. 2 and 3.

Calculations show that for a body with a two-wedge cross section, increasing the thickness ratio leads to a continuous decline of the lift effectiveness (Fig. 2). For other configurations, increasing the rib thickness (β) for a specified number of prongs ($n \geq 3$) initially causes a decline of the lift effectiveness of the body. However, as the configuration of the cross section approaches a regular convex polygon with n sides, the decrease in \bar{C}_n^α stops, to be followed by a certain increase (Fig. 3). The values of \bar{C}_n^α for the cases of a regular n -sided polygon are indicated by points in this figure.

Let us now examine configurations whose cross sections are formed by arcs of circles (Fig. 1, d and e). In this case, the exterior of the contour is

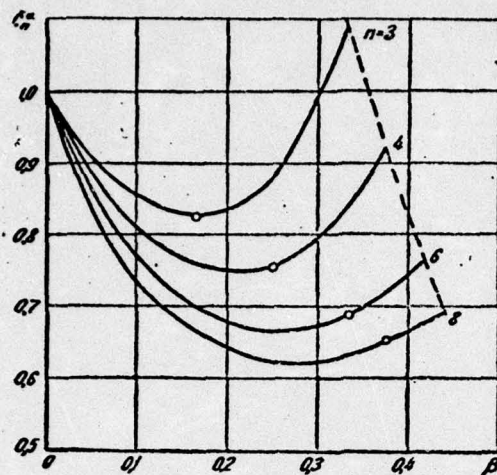


FIGURE 3

mapped onto the exterior of a circle of radius r by means of the following function:⁴

$$\frac{2z-L}{2z+L} = \left[\frac{4(1-\beta)\zeta-L}{4(1+\beta)\zeta+L} \right]^{2(1-\beta)}. \quad (17)$$

For different shapes of the cross-sectional contour, the radius r of the mapped circle will be different. In addition, the mapped circle intersects the real axis at points with coordinates $(\pm \frac{L}{4(1-\beta)}, 0)$, and its center may be shifted along the imaginary axis. Here $2\beta\pi$ is the angle between the arcs of circle tangent at the point of intersection; the parameter β changes between the limits $0 \leq \beta \leq \frac{1}{2}$. This contour is characterized by thickness c and concavity of the cross section in fractions of the span L . From these quantities, one can readily determine all the remaining parameters of the cross section and the radius of the mapped circle:

$$\beta = \frac{1}{\pi} \arctg \frac{2c}{1+4f^2-c^2}; \quad (18)$$

$$\frac{S_0}{L^2} = \frac{1}{8} \left\{ \frac{2c(1+4f^2-c^2)}{4f^2-c^2} + \frac{[1+(2f+c)^2]^2}{(2f+c)^2} \arctg(2f+c) - \right. \\ \left. - \frac{[1+(2f-c)^2]^2}{(2f-c)^2} \arctg(2f-c) \right\}; \quad (19)$$

$$r = \frac{L}{4(1-\beta) \sin \alpha}, \quad (20)$$

where

$$\alpha = \frac{\pi - 2 \arctg(2f+c)}{2\pi(1-\beta)}.$$

The expansion of the function in the vicinity of an infinitely distant point is

$$z = \zeta + \frac{4(1-\beta)^2-1}{48(1-\beta)^2} \cdot \frac{L^2}{\zeta} + \dots \quad (21)$$

Hence

$$\operatorname{Re}(a_1) = \frac{4(1-\beta)^2-1}{48(1-\beta)^2} L^2.$$

Consequently, the expressions for the apparent mass and for the coefficient C_n^α may be written as follows:

$$m = \frac{\pi \rho L^3}{8} \left[\frac{1}{(1-\beta)^2 \sin^2 \alpha \pi} + \frac{4(1-\beta)^2 - 1}{3(1-\beta)^2} - \frac{8 S_0}{\pi L^2} \right]; \quad (22)$$

$$C_n^\alpha = \frac{\pi \lambda}{2} \frac{1}{2} \left[\frac{1}{(1-\beta)^2 \sin^2 \alpha \pi} + \frac{4(1-\beta)^2 - 1}{3(1-\beta)^2} - \frac{8 S_0}{\pi L^2} \right]. \quad (23)$$

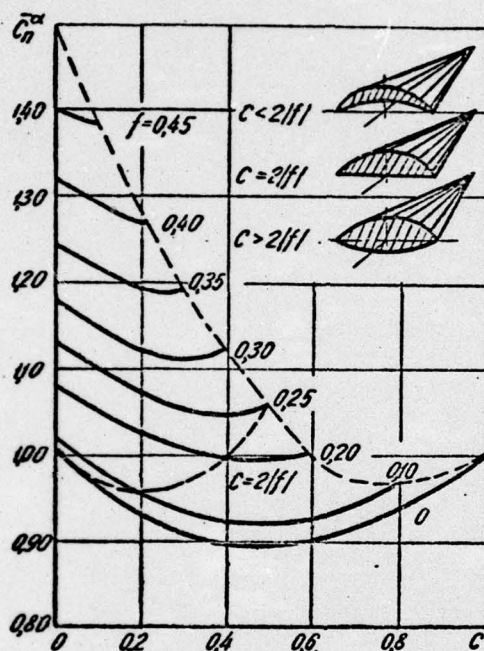


FIGURE 4

We introduce the relative coefficient $\bar{C}_n^\alpha = \frac{C_n^\alpha}{C_{n0}^\alpha}$, where $C_{n0}^\alpha = \frac{\pi \lambda}{2}$ is the characteristic of a planar wing. The function $\bar{C}_n^\alpha = \bar{C}_n^\alpha(c, f)$ with $c \leq 1 - 2|f|$ is plotted in Fig. 4.

The results of the calculations show that the lift effectiveness of the bodies studied is considerably affected by the concavity of the cross section and, to a lesser extent, by the thickness ratio. Moreover, if $|f| > 0.3$,

\bar{C}_n^α decreases with increasing thickness ratio, and if $|f| < 0.3$, the function $\bar{C}_n^\alpha = \phi(c, f)$ has a minimum.

The results of the present study, obtained in terms of the thin body theory, can also be applied to an estimation of the lift effectiveness of "nonthin" configurations if the relative dependences of \bar{C}_n^α are used, provided that the exact values of the coefficients C_{n*}^α and C_{n0}^α are known.

REFERENCES

/10

1. Gonor, A. L., M. N. Kazakov and A. I. Shvets, Measurement of the drag of a star-shaped body in supersonic flow at Mach numbers 6 and 8. *Mekhanika zhidkosti i gaza*, Izv. AN SSSR, No. 1, 1968.
2. Maykapar, G. I., Optimum shape of lifting bodies at hypersonic velocities. *Mekhanika zhidkosti i gaza*, Izv. AN SSSR, No. 2, 1967.
3. Nielsen, J., *Aerodynamics of Guided Missiles*, Oborongiz Publishing House, Moscow, 1962.
4. Lavrent'yev, M. L. and V. V. Shabat, *Methods of the Theory of Functions of a Complex Variable (Metody teorii funktsiy kompleksnogo peremennogo)*, Fizmatgiz Publishing House, Moscow, 1958.
5. Kholyavko, V. I., Aerodynamic characteristics of nonplanar airfoils in terms of the thin body theory, in: *Aircraft Construction and Technology of the Air Fleet (Samoletostroyeniye i tekhnika vozdushnogo flota)*, No. 11, Khar'kov State University Publishing House, Khar'kov, 1967.